Cell Host & Microbe
Article

Tetherin/BST-2 Is Essential for the Formation of the Intracellular Virus-Containing Compartment in HIV-Infected Macrophages

Hin Chu,[1] Jaang-Jiun Wang,[1] Mingli Qi,[1] Jeong-Joong Yoon,[1] Xuemin Chen,[1] Xiaoyun Wen,[1] Jason Hammonds,[1] Lingmei Ding,[1] and Paul Spearman[1,*]
[1]Emory University Department of Pediatrics and Children's Healthcare of Atlanta, Atlanta, GA 30322, USA
*Correspondence: paul.spearman@emory.edu
http://dx.doi.org/10.1016/j.chom.2012.07.011

SUMMARY

HIV-1 assembly and release occur at the plasma membrane in T lymphocytes, while intracellular sites of virus assembly or accumulation are apparent in macrophages. The host protein tetherin (BST-2) inhibits HIV release from the plasma membrane by retaining viral particles at the cell surface, but the role of tetherin at intracellular HIV assembly sites is unclear. We determined that tetherin is significantly upregulated upon macrophage infection and localizes to an intracellular virus-containing compartment (VCC). Tetherin localized at the virus-VCC membrane interface, suggesting that tetherin physically tethers virions in VCCs. Tetherin knockdown diminished and redistributed VCCs within macrophages and promoted HIV release and cell-cell transmission. The HIV Vpu protein, which downregulates tetherin from the plasma membrane, did not fully overcome tetherin-mediated restriction of particle release in macrophages. Thus, tetherin is essential for VCC formation and may account for morphologic differences in the apparent HIV assembly sites in macrophages versus T cells.

INTRODUCTION

Human immunodeficiency virus type 1 (HIV-1) assembly occurs predominantly at the plasma membrane of infected T lymphocytes and model epithelial cell lines (Chu et al., 2009; Finzi et al., 2007; Gelderblom, 1991; Jouvenet et al., 2006; Ono and Freed, 2004). In contrast, infected macrophages examined by electron microscopy and immunofluoresent microscopic techniques demonstrate an intense intracellular accumulation of virions in a compartment marked by characteristic components of the multivesicular body (MVB), including CD81, CD9, MHC class II, and CD63 (Nydegger et al., 2003; Pelchen-Matthews et al., 2003; Raposo et al., 2002; Sherer et al., 2003). The presence of apparent assembly in intracellular sites with characteristics of the MVB in macrophages led to models for HIV-1 assembly in which the endocytic network plays an important role. Some models for HIV-1 assembly in macrophages propose that intracellular assembly predominates, with release from the intracellular compartment across the virologic synapse upon contact with T cells (Gousset et al., 2008; Groot et al., 2008; Montaner et al., 2006). Defining the precise site of assembly in the macrophage and the factors determining the apparent intracellular assembly site thus has relevance to a number of areas of HIV biology.

Jouvenet and coworkers previously suggested that the plasma membrane was the only site of HIV assembly in infected macrophages, and that HIV particles observed in the intracellular compartments resulted from endocytosis of viral particles from the cell surface (Jouvenet et al., 2006). Tetherin was subsequently identified as an important HIV restriction factor resulting in the retention of particles at the plasma membrane of cells and leading to enhanced endocytosis of particles in model cell lines (Neil et al., 2008). Tetherin, also known as BST-2 or CD317, is an unusual type II membrane protein that localizes to lipid rafts and is endocytosed through a clathrin- and AP2-dependent mechanism (Masuyama et al., 2009; Rollason et al., 2007). Tetherin is highly concentrated at the particle budding site in T cell lines and plays a physical tethering role in retaining strings of virions in cells infected with Vpu-deficient virus (Hammonds and Spearman, 2009; Hammonds et al., 2010; Perez-Caballero et al., 2009). Vpu overcomes the restrictive effects of tetherin, resulting in enhanced particle release. The mechanism of Vpu's action in counteracting tetherin remains to be fully elucidated, but retention of tetherin at intracellular sites, downregulation of tetherin from the cell surface, and enhanced degradation of tetherin through lysosomal and/or proteasomal pathways have all been reported to play important roles (Douglas et al., 2009; Dube et al., 2010; Goffinet et al., 2009; Iwabu et al., 2009; Mangeat et al., 2009; Mitchell et al., 2009; Van Damme et al., 2008).

Here we investigated the role of tetherin in primary human macrophages using immunofluorescence and electron microscopic methods, in order to define the role of tetherin in the virus-containing compartment (VCC). Tetherin was markedly upregulated following macrophage infection, and relief of restriction of particle release by Vpu was incomplete. Remarkably, VCCs in infected macrophages were highly enriched in tetherin, and depletion of tetherin caused a dramatic reduction and redistribution of the VCC. Along with this redistribution, we observed enhanced transmission of virus from macrophages to T cells upon tetherin depletion.

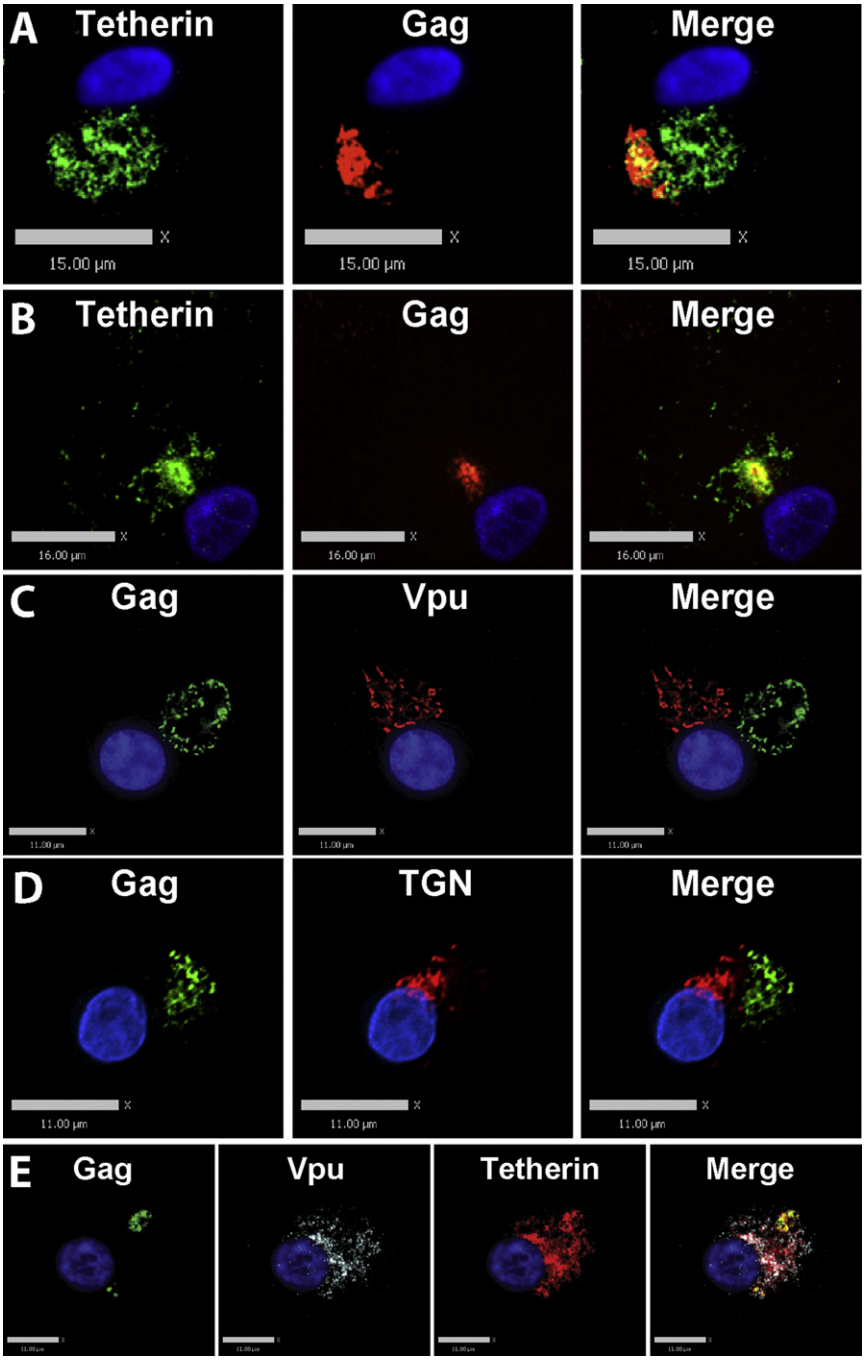

Figure 1. Tetherin Is Highly Concentrated in Virus-Containing Compartments within HIV-1-Infected MDMs

(A) MDMs were infected with VSV-G-pseudotyped HIV-1 R8-BaL. Eight days postinfection, cells were fixed and immunolabeled for HIV-1 Gag (red, anti-CA183) and tetherin (green, anti-tetherin). Bars represent 15 µm.

(B) MDMs were infected with HIV-1 BaL biological stock. Eight days postinfection, cells were fixed and immunolabeled for HIV-1 Gag (red, anti-CA183) and tetherin (green, anti-tetherin). Bars represent 16 µm.

(C–E) MDMs were infected with VSV-G-pseudotyped HIV-1 R8-BaL for 8 days followed by fixation, permeabilization, and immunostaining for Vpu (red, anti-Vpu) and Gag (green, anti-CA183) in (C); for TGN (red, anti-TGN) and Gag (green, anti-CA183) in (D); and for Vpu (cyan, anti-Vpu), Gag (green, anti-CA183), and tetherin (red, anti-tetherin) in (E). Bars represent 11 µm. See also Figure S1.

RESULTS

Tetherin Is Highly Concentrated in Virus-Containing Compartments within HIV-1-Infected MDMs

We hypothesized that tetherin may play a role in the formation of VCCs in HIV-infected macrophages. To test this hypothesis, we first examined the subcellular localization of tetherin in MDMs. In HeLa and other epithelial cell lines, tetherin is found within the trans-Golgi network (TGN), within recycling endosomes, and at the plasma membrane, without significant concentration in late endosomes (Dube et al., 2009; Habermann et al., 2010; Le Tortorec and Neil, 2009). In HIV-infected MDMs, we observed tetherin on the cell surface as well as in large intracellular compartments (Figure 1). We noted that tetherin was highly concentrated in intracellular compartments and often appeared as more than a single population in the cell (Figure 1A). Infected MDMs double-labeled for tetherin and Gag demonstrated a substantial level of colocalization between the two proteins (Figure 1A). The colocalization appeared to occur within a subset of tetherin-rich compartments and was consistently observed in macrophages from multiple donors. To confirm this result, we repeated the experiment using a biological stock of nonpseudotyped HIV-1 BaL instead of VSV-G-pseudotyped virus and obtained identical results (Figure 1B). In parallel, we also performed the same experiment but replaced the tetherin primary antibody with prebleed serum from the same animal or omitted the primary antibody. In both of these controls, we failed to observe staining of this compartment (data not shown). It has been reported previously that HIV-1 Vpu colocalizes with tetherin in the TGN of infected cells (Dube et al., 2009; Le Tortorec and Neil, 2009). In addition, HIV-1 Vpu may counteract tetherin by sequestering tetherin in the TGN (Dube et al., 2009, 2010; Le Tortorec and Neil, 2009). To examine the possibility of potential interactions between Gag, Vpu, and tetherin in infected MDMs, we performed a series of immunostaining studies and documented the cellular distribution of Gag, Vpu, and tetherin in infected MDMs. We first double-labeled MDMs with antibodies against Gag and Vpu or Gag and TGN. Gag and Vpu were found within distinct compartments in infected MDMs,

with no detectable colocalization between the two (Figure 1C). The VCC identified by Gag antibody staining was entirely distinct from the TGN (Figure 1D). We then performed a triple staining experiment in which tetherin, Gag, and Vpu were labeled. Tetherin was found in two compartments inside the cell, one that colocalized with Gag (the VCC) and another that colocalized with Vpu (the TGN) (Figure 1E). As an additional control, we examined the distribution of tetherin and protein disulphide isomerase (PDI), an ER marker. Tetherin did not colocalize with PDI (see Figure S1 online).

Tetherin Colocalizes with Markers of Two Distinct Intracellular Compartments in MDMs: The Multivesicular Body and TGN

To further define the exact compartments in which tetherin and HIV-1 Gag colocalize, we performed immunostaining for tetherin and various cellular markers in both uninfected and HIV-infected MDMs. Cellular markers that we tested included CD81, CD9, CD63, and LAMP-1, as well as the TGN marker TGN46 and ER marker PDI as described above.

In uninfected MDMs, we observed a significant level of colocalization between tetherin and both of the MVB markers, CD81 and CD9 (Figure 2A and Figure S1, with quantitation in Figure 2C). We noticed that although the vast majority of CD81 and CD9 colocalized with tetherin, only a subset of intracellular tetherin colocalized with CD81 and CD9. At the same time, we again detected a substantial but partial colocalization between tetherin and the TGN marker, TGN46 (Figure 2A). These results indicate that in uninfected macrophages, tetherin resides in two distinct compartments in MDMs: the TGN and the CD81/CD9-positive endosome. Interestingly, immunostaining performed for CD63 and LAMP-1 in uninfected MDMs failed to identify a significant colocalization between tetherin and these late endosome/MVB markers (Figure 2A, CD63 and LAMP-1 rows). LAMP-1 and CD63 were located in close proximity but did not directly overlap with tetherin in these uninfected cells.

Next, we examined HIV-infected MDMs for the same set of markers. We observed a strong colocalization between a subset of intracellular tetherin and the tetraspanins CD81 and CD9, similar to what had been seen in uninfected macrophages (Figure 2B and Figure S1). In contrast to the uninfected cells, however, immunostaining for CD63 and LAMP-1 in infected MDMs revealed a significantly enhanced level of colocalization between CD63, LAMP-1, and tetherin (Figure 2B, CD63 and LAMP-1 rows). The pattern of colocalization between tetherin and CD63 or LAMP-1 was similar to what we observed between tetherin and CD81/CD9, such that a subpopulation of tetherin colocalized almost completely with the intracellular CD63 or LAMP-1. HIV infection therefore led to an enrichment of CD63 and LAMP1 in the tetherin/CD9/CD81-rich compartment, reminiscent of previously reported findings that HIV alters this compartment (Deneka et al., 2007).

To quantify these observations, we measured the partial colocalization coefficients (M_x and M_y) between tetherin and each cellular marker using the colocalization function of Volocity 5.2.1 (Manders et al., 1993). Infected and uninfected macrophages demonstrated a high degree of colocalization for CD81, CD9, and TGN with tetherin (Figure 2C), while ER colocalization was minimal, consistent with the impression from individual images. HIV-1 infection increased the degree of colocalization of CD63 and LAMP-1 with tetherin as indicated by a significant increase ($p < 0.0001$) in colocalized pixels (Figure 2C). In infected MDMs, the M_y values for the degree colocalization of CD63 and LAMP-1 with tetherin were increased by ~3-fold in comparison with uninfected MDMs.

Triple staining for Gag, tetherin, and cellular compartment markers confirmed that a substantial intracellular subset of tetherin colocalized with HIV-1 Gag in CD81- and CD63-enriched VCCs, and that a separate population of tetherin was found in the TGN (Figure S2). In contrast with the strong colocalization between Gag and tetherin ($M_y = 0.75 \pm 0.18$), the level of colocalization between Gag and ER was minimal ($M_y = 0.09 \pm 0.04$). The level of colocalization between Gag/ER and Gag/tetherin was significantly different ($p < 0.0001$). Altogether, these results indicate that in HIV-infected MDMs, tetherin resides in two distinct compartments: the TGN, where it colocalizes with Vpu; and the VCC, where it colocalizes with Gag and markers of the MVB.

Tetherin Links Virions to the Limiting Membranes of Virus-Containing Compartments in Human Macrophages

We and others recently demonstrated that tetherin forms a link between chains of extracellular virions and the plasma membrane on the surface of the A3.01 T cell line (Hammonds et al., 2010) or HeLa cells (Fitzpatrick et al., 2010). We next sought to examine the location of tetherin at the ultrastructural level in human macrophages using immuno-EM techniques. Infected macrophages were fixed, embedded in resin, and prepared for thin sections, followed by postembedding immunogold labeling using anti-tetherin antiserum or preimmune control sera as the primary antibody. We found only rare gold particles in the cytoplasm of cells outside of the VCCs, while the presence of beads between numerous virion particles within the VCCs was evident (Figures 3A–3C). As in our previous report examining extracellular particle tethering, some extended filamentous strings studded with tetherin were evident in the VCC (Figures 3D and 3E). More frequently, tetherin was identified at the interface between particles (Figures 3F, 3H, 3I). Tetherin was also prominently found connecting particles to the periphery of the compartment, an apparent connection with the limiting membrane (Figures 3E–3G). The specificity of labeling of the VCC was confirmed by a low background rate of nanogold particles within the compartments when preimmune rabbit serum was employed (Figure 3J–3L). Purity of macrophages utilized in these and other experiments was greater than 91% (Figure S3).

Tetherin Expression Is Upregulated Following Infection of MDMs and Is Incompletely Downregulated by Vpu

Particle output from MDMs is enhanced following infection with viruses bearing an intact *vpu* gene (Balliet et al., 1994; Schubert et al., 1995), suggesting that Vpu's antagonism of tetherin is functional in this cell type. We similarly documented an increase in p24 release over time from MDMs following infection with NL4-3 versus NLUdel (Figure 4A). This difference was very reproducible and was seen in MDMs from multiple different donors. Remarkably, cellular tetherin levels increased following infection

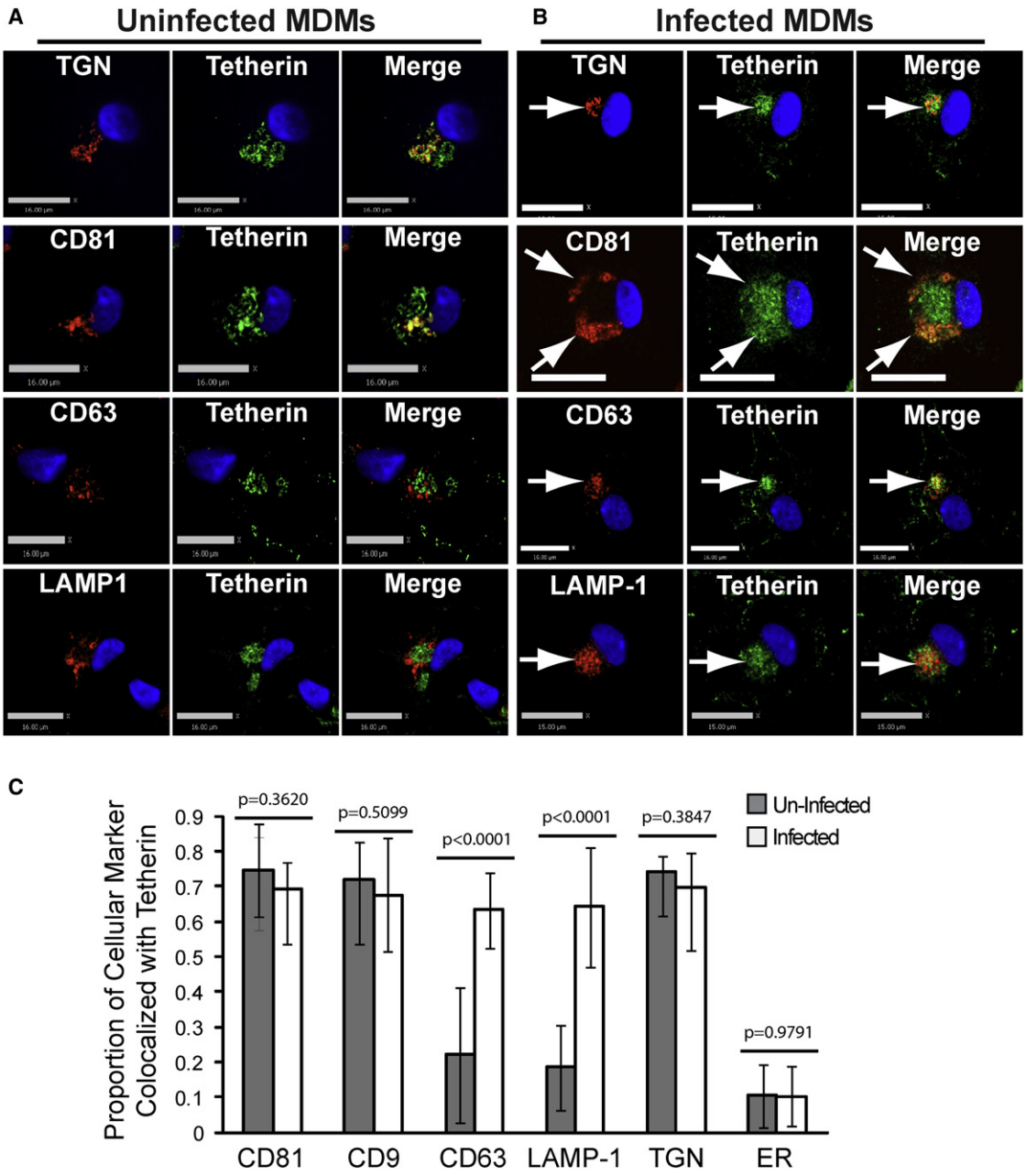

Figure 2. Subcellular Distribution of Tetherin in Uninfected MDMs

(A) Uninfected MDMs were fixed and immunolabeled for cellular markers (red, anti-TGN46, anti-CD81, anti-CD63, and anti-LAMP-1) and tetherin (green, anti-tetherin). Note lack of colocalization with CD63 and LAMP-1. Bars represent 16 μm. Images selected are representative of the major findings from more than 100 cells examined in five independent experiments.

(B) MDMs were infected with VSV-G-pseudotyped HIV-1 NL4-3. Eight days postinfection, cells were fixed and immunolabeled for cellular markers (red, anti-TGN46, anti-CD81, anti-CD63, and anti-LAMP-1) and tetherin (green, anti-tetherin). Bars represent 15 μm for LAMP-1 panel and 16 μm for the remaining panels.

(C) Quantitation of colocalization between cellular marker and tetherin in uninfected (filled bars) or infected (white bars) MDMs. The partial correlation coefficient and standard deviation shown represent the degree of colocalization derived from images of at least ten representative cells. Results were shown as mean ± SD. Statistical comparison between the groups were performed by unpaired t test using GraphPad Prism 5. See also Figure S2.

and remained elevated over baseline for more than 6 days in macrophages following infection with either NL4-3 or NLUdel (Figure 4B). The magnitude and timing of upregulation varied slightly from donor to donor, but the upregulation was detectable in every donor examined (n > 10). The use of VSV-G itself was not the stimulus for tetherin upregulation, as supernatants from VSV-G-transfected cells did not enhance tetherin expression (Figure S4A). To further verify this, we infected MDMs from multiple donors with PBMC-propagated HIV-1 BaL without pseudotyping, and confirmed that the upregulation was

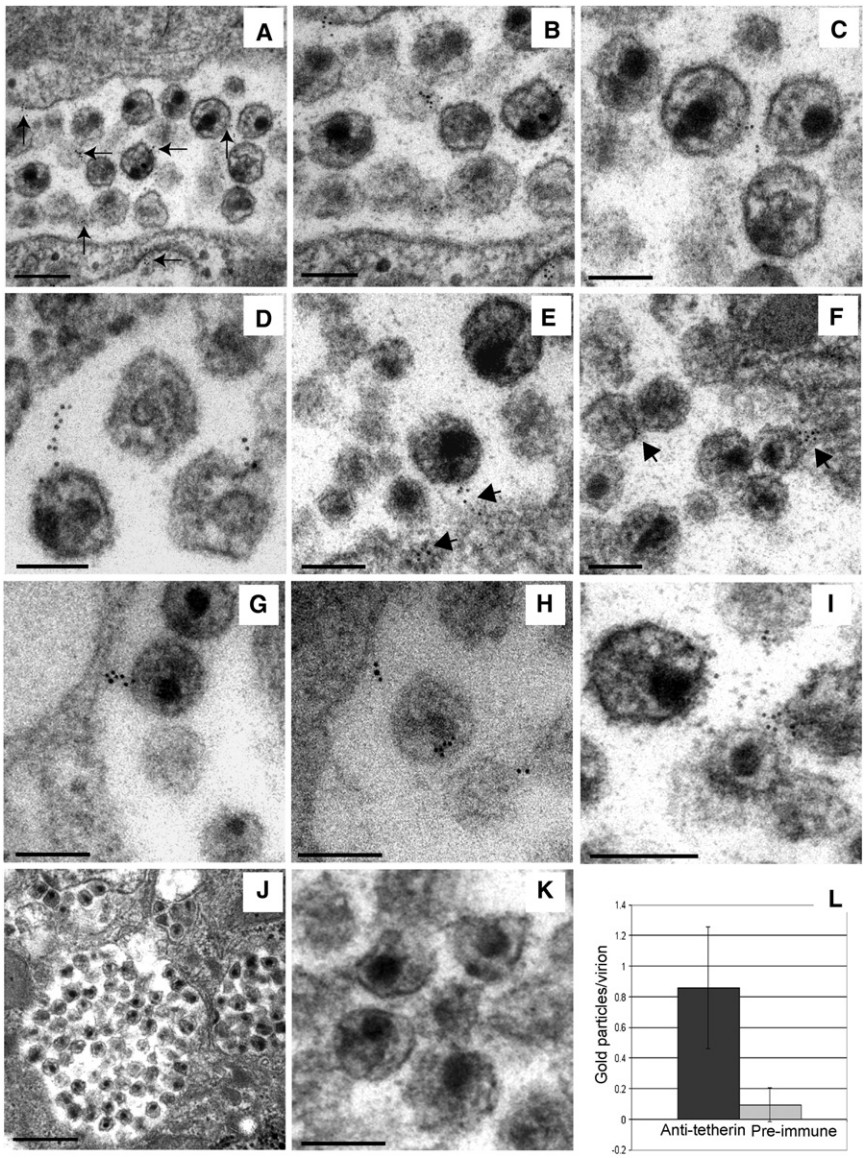

Figure 3. Immunoelectron Microscopic Localization of Tetherin within the Virus-Containing Compartment in Macrophages

MDMs were infected with VSV-G-pseudotyped HIV-1 NL4-3. Cells were harvested at day 8, fixed, embedded, and sectioned. Sections were etched with H_2O_2 and labeled with 6 nm gold beads using anti-tetherin antisera using methods previously established (Hammonds et al., 2010).

(A) Multiple nanogold beads between particles at low power within a VCC; bar, 200 nm. Arrows were added to point out beads.

(B) Higher-magnification view of left half of (A); bar, 100 nm.

(C) Higher-magnification view of upper right portion of (A); bar, 100 nm.

(D) Extended tether and beads between particles; bar, 100 nm.

(E) Tetherin at base of particles, between limiting membrane and particles within intracellular compartment in macrophages. Bar, 100 nm.

(F) Tetherin immunolabeling at base of particle and between particles within intracellular compartment in macrophages. Bar, 100 nm.

(G) Tetherin linking particle to the limiting membrane of a VCC; bar, 100 nm.

(H and I) Additional views of tetherin labeling within VCCs, on surface of virions and between virions.

(J) VCC, control section employing preimmune serum and immunogold labeling otherwise identical to that in (A)–(I). Bar, 500 nm.

(K) Detail of same VCC as in (J) with control (preimmune) labeling; bar, 100 nm.

(L) Gold particles found within VCCs of HIV-infected macrophages, mean ± SD, using specific anti-tetherin sera (black) or pre-immune sera (gray). Twenty consecutive VCCs with virions were assessed for each label, and normalized by total number of visualized particles. See Figure S3 for assessment of macrophage purity by flow cytometry.

observed following infection with this R5-tropic virus (Figure 4C). The increase in total cellular tetherin was diminished but not prevented by Vpu, as tetherin levels at day 8 to day 12 postinfection were greater in cells infected with NLUdel than in those infected with NL4-3. Quantitative analysis of western blots confirmed a consistent upregulation of tetherin in HIV-1-infected MDMs from multiple donors (Figure S4B). In stark contrast to the phenotype seen in HeLa cells, cell-surface levels of tetherin in MDMs were not diminished following infection with NL4-3 but actually increased (Figure 4D). Vpu failed to prevent the increase in cell surface tetherin levels as indicated in repeated experiments by the increased mean fluorescence intensity of surface-stained cells (Figure 4D, lower right). In individual experiments, the increase in cell-surface tetherin was greater when MDMs were infected with NLUdel, although taken together the difference was not statistically significant (Figure 4D, lower right). In parallel, we infected HeLa cells with the same viruses and observed a significant decrease in cell-surface tetherin following NL4-3 but not NLUdel infection (Figure 4D, HeLa). These results indicate that although Vpu does enhance particle release from MDMs, Vpu's ability to downregulate tetherin in MDMs is incomplete as compared with model cell lines such as HeLa. Furthermore, Vpu is unable to prevent the upregulation of cellular tetherin expression that occurs following infection with HIV. We also measured total tetherin levels by flow cytometry, and this approach confirmed that total tetherin is upregulated in MDMs in a similar manner to the surface upregulation (Figures S4C–S4E, right panels), while NL4-3-infected HeLa cells demonstrated a decrease in both surface and total tetherin levels (Figures S4C–S4E, left panels).

Tetherin Knockdown Promotes Particle Release from HIV-Infected MDMs Even in the Presence of Vpu

The colocalization and immuno-EM data described above demonstrated that tetherin is enriched within the VCC in macrophages and appears to tether virions in this compartment. To

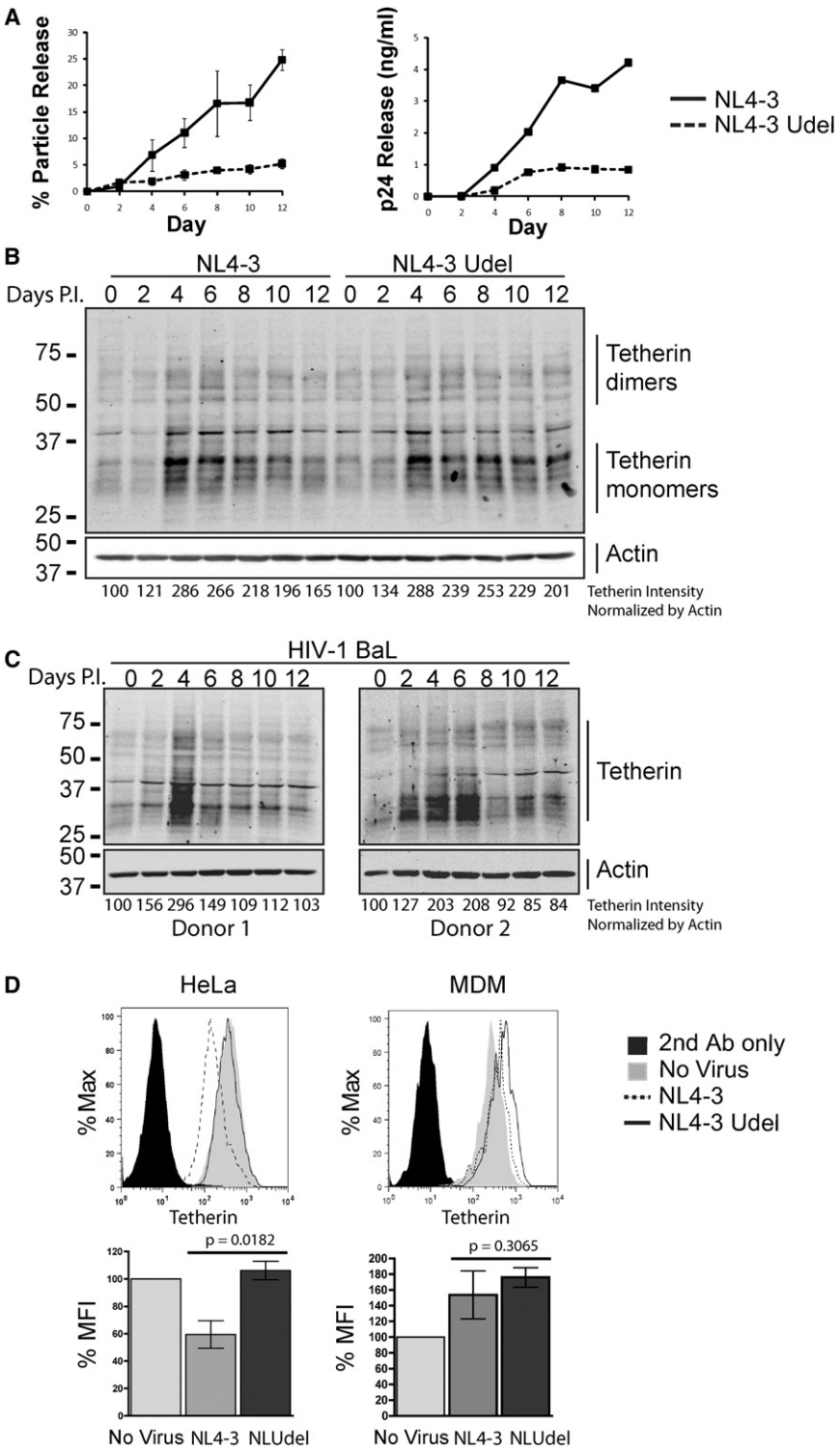

Figure 4. Vpu and Tetherin in Infected MDMs

(A) Particle release from MDMs was assessed over time using a p24 antigen ELISA. The efficiency of release was plotted as percentage of extracellular p24/total p24 from three experiments. The majority of p24 was retained in macrophages infected with either NL4-3 or NLUdel, and total amounts of p24 (cell + sup) were similar. Right-sided graph represents one of the experiments, presented as released p24 antigen. Error bars represent SD.

(B) Western blot of tetherin and actin over time following infection of MDMs.

(C) Western blot of tetherin and actin over time from MDMs infected with HIV-1 BaL. MDMs were infected with HIV-1 BaL, and cell lysates were harvested at the indicated time points. Western blots were performed as mentioned above. Results from two donors were shown as representatives of five independent experiments.

(D) Cell-surface levels of tetherin following infection with NL4-3 (dashed line) or NLUdel (solid line). Cells were stained with anti-p24 antibody to allow gating on the infected population. Results of individual experiments in HeLa (left) and MDMs (right) are shown. Below are %MFI with error bars representing SD at 48 hr postinfection (HeLa) or 4 days postinfection (MDMs), with results from three independent experiments plotted. Statistical comparison between the groups was performed by unpaired t test using GraphPad Prism 5. See also Figure S4.

examine the functional role of tetherin, we depleted endogenous tetherin in MDMs using siRNA and measured the effects on particle output and on the volume of the VCC. Figure 5A is a representative example of the tetherin knockdown achieved, in which the MDMs were first treated with tetherin or control siRNA three times to achieve a potent depletion of endogenous tetherin, followed by NL4-3 infection. The tetherin level in MDMs was significantly reduced (70%–80%) and persisted for the time span of the experiment (Figure 5A). As demonstrated in the control knockdown cells, control siRNA and the siRNA transfection reagent did not affect tetherin expression in MDMs, which increased after infection (Figure 5A).

We then analyzed the efficiency of particle release in siRNA-treated, HIV-infected MDMs. NLUdel was very poorly released from MDMs transfected with control siRNA (Figure 5B, open diamonds). In contrast, following tetherin depletion, particle release of NLUdel was significantly increased (Figure 5B, closed diamonds). Interestingly, the level of NLUdel release in tetherin knockdown MDMs was comparable to the level of NL4-3 release in control knockdown MDMs (Figure 5B, compare closed diamonds and open squares). Although NL4-3 release from MDMs was greater than that of NLUdel, tetherin depletion had a clear added effect on particle release (Figure 5B, closed squares). The additive effect of tetherin knockdown and Vpu in particle release from infected MDMs for NL4-3 confirmed our

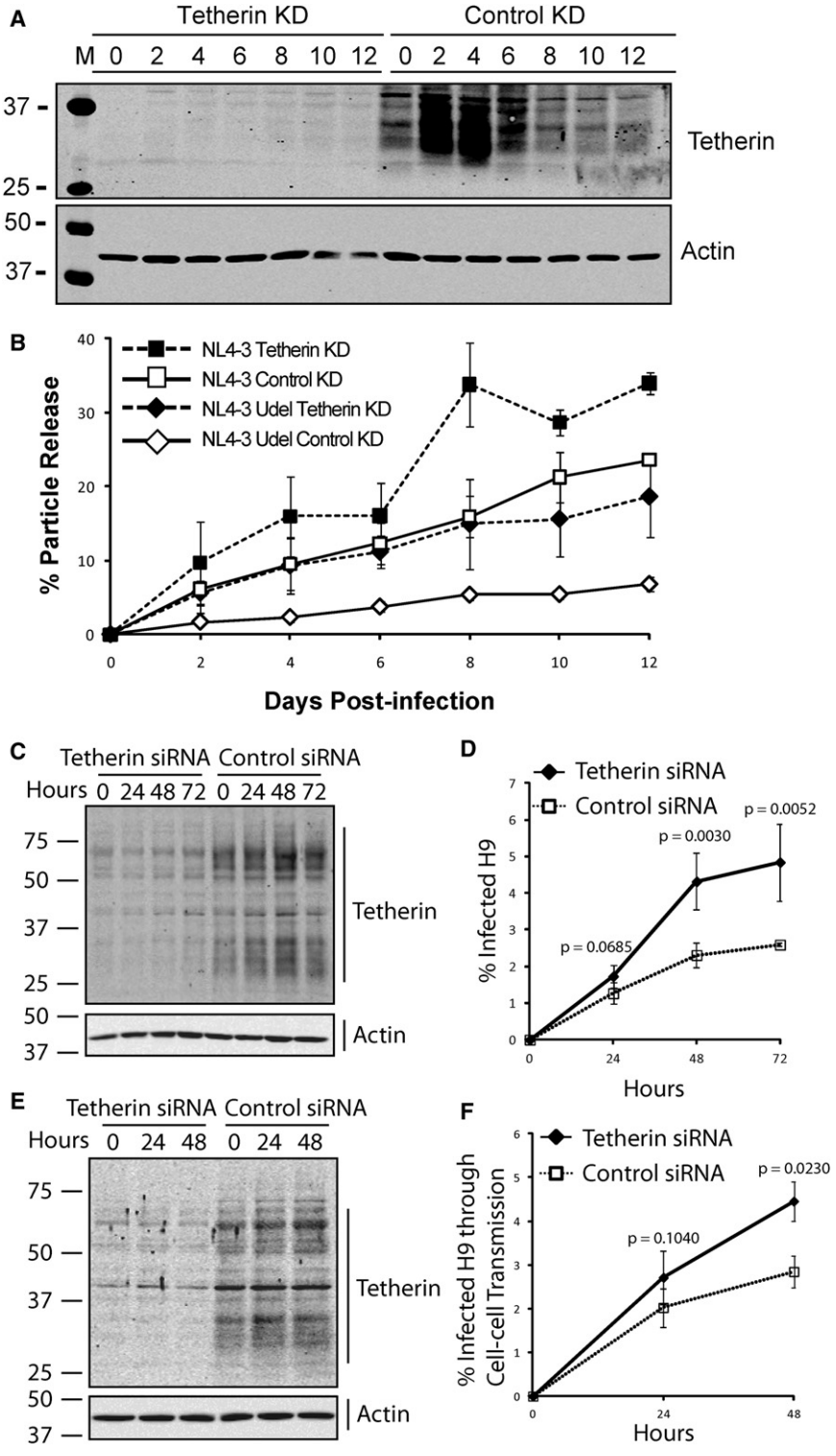

Figure 5. Effects of Tetherin Knockdown on Particle Release and Cell-Cell Transmission from MDMs

(A) MDMs were transfected with tetherin siRNA or control siRNA three times followed by NL4-3 infection. Infected cells were harvested at indicated time points postinfection, lysed, and analyzed by western blotting using rabbit anti-tetherin or mouse anti-actin antiserum.

(B) Particle release from tetherin siRNA or control siRNA treated and infected MDMs was assessed over time using a p24 antigen ELISA. The efficiency of release is plotted as percentage of extracellular p24/total p24 from three experiments, with standard deviations indicated.

(C) Western blot of tetherin and actin from MDMs in cell-cell transmission assays. MDMs were treated with control or tetherin siRNA followed by NL4-3 infection.

(D) H9 cells in contact with infected MDMs were harvested and fixed at the indicated time points, followed by labeling for CD3 and HIV-1 Gag. Flow cytometry was performed to analyze the percentage of infected H9 cells by gating on Gag- and CD3-positive cells. Error bars represent SD.

(E) Western blot of tetherin and actin of MDMs in cell-cell transmission assays using the Transwell system.

(F) H9 cells were harvested from the insert chambers and the bottom chambers separately and labeled for CD3 and HIV-1 Gag. Flow cytometry was performed to analyze the percentage of H9 cells that were CD3 and Gag positive. Cell-cell transmission events were derived by subtracting the cell-free transmission events from the total transmission events. Error bars represent SD. Statistical comparison between the groups was performed by unpaired t test using GraphPad Prism 5.

earlier finding that Vpu was unable to efficiently counteract the effect of tetherin in infected MDMs, and that residual restriction of release by tetherin remained.

Currently the role of tetherin in cell-cell transmission remains incompletely defined. To elucidate the role of tetherin in cell-cell transmission from infected MDMs, we first performed a transmission assay to evaluate cell-cell transmission by gently centrifuging H9 T cells onto an adherent monolayer of infected MDMs and quantifying infected H9 cells by flow cytometry. Tetherin siRNA treatment successfully inhibited tetherin expression in the donor MDMs (Figure 5C). H9 cells that were cocultured in contact with tetherin siRNA-treated MDMs were infected at a higher efficiency compared with H9 cells cocultured with control siRNA-treated MDMs (Figure 5D). At 72 hr after the coculture, 4.8% ± 1.04% of H9 cells cocultured with tetherin siRNA-treated MDMs were infected, compared with 2.6% ± 0.05% of H9 cells cocultured with control siRNA-treated MDMs (Figure 5D). This experiment suggested to us that tetherin knockdown promoted cell-cell transmission from infected MDMs to H9 cells, although some cell-free transmission was also possible by this method. Next, we employed a Transwell cell-culture system and refined our cell-cell transmission study.

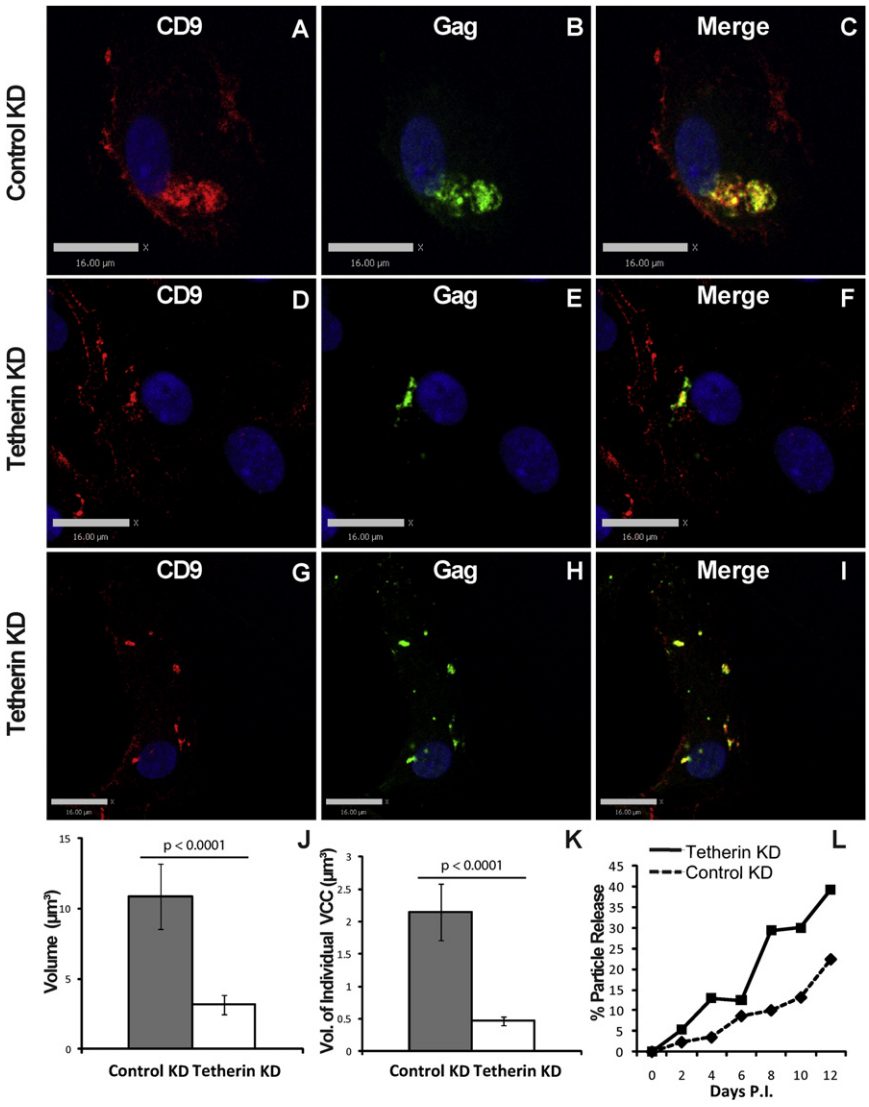

Figure 6. Effect of Tetherin Knockdown on the Virus-Containing Compartments in MDMs

(A–C) MDMs were transfected with control siRNA three times followed by infection with VSV-G-pseudotyped NL4-3. At day 4 postinfection, cells were fixed and immunolabeled for CD9 (red, anti-CD9) and HIV-1 Gag (green, anti-CA183). Bars, 16 μm.

(D–I) MDMs were transfected with tetherin siRNA three times followed by infection with VSV-G-pseudotyped NL4-3. At day 4 postinfection, cells were fixed and immunolabeled for CD9 (red, anti-CD9) and HIV-1 Gag (green, anti-CA183). Bars, 16 μm.

(J) Quantitation of the volume of the VCCs in infected MDMs with tetherin knockdown or control knockdown. The volume of the VCCs within each cell for 30 cells was calculated using the Volocity 5.5.1 measurements module.

(K) Quantitation of the volume of individual VCCs within infected MDMs with tetherin knockdown or control knockdown. Colocalized pixels between CD9 and Gag were determined as above and volumes calculated for individual VCCs, counting 150 VCCs for each arm of the experiment. Error bars in (J) and (K) represent SD.

(L) Particle release from MDMs from the same donor in the experiment presented here was assessed over time using a p24 antigen ELISA.

Tetherin Knockdown Inhibits the Formation of the Virus-Containing Compartments in Infected MDMs

In order to investigate the effect of tetherin knockdown on the VCCs in infected MDMs, we applied quantitative confocal microscopy on the siRNA-treated, HIV-infected MDMs. MDMs were treated with tetherin siRNA or control siRNA followed by NL4-3 infection, and harvested at day 4 postinfection. HIV Gag colocalization with CD9 was used as a measure of the VCC, and the volume of the VCC was measured using 3D image reconstructions of the Gag and CD9 colocalized pixels. Control siRNA-treated MDMs visually resembled untreated MDMs, with large collections of Gag colocalizing with CD9 in the VCC (Figures 6A–6C). Remarkably, the location and size of the VCC were altered in tetherin-depleted MDMs. In these cells, the VCC size was diminished, and when present was found as smaller (Figures 6D–6F) and often more peripheral puncta (Figures 6G–6I). The average volume of the VCCs measured from 30 control siRNA-treated MDMs on day 4 following infection was 10.9 μm^3, while the average volume of the VCCs in tetherin-depleted MDMs was dramatically reduced to 3.2 μm^3 (Figure 6J). This measurement was performed using total (per cell) VCC volume. We also examined the average volume of the individual VCCs, and these results confirmed the marked reduction in size of the individual VCCs upon tetherin depletion (Figure 6K). These results indicate that depletion of tetherin markedly reduces the size and alters the distribution of the VCCs in MDMs. Tetherin knockdown in these experiments

In this set of experiments, control or tetherin siRNA-treated MDMs in Transwell plates were first infected with HIV, followed by addition of H9 cells to the top chamber (no MDMs) or the bottom chamber (in contact with MDMs) on day 2 postinfection. Infected H9 cells detected from the top chamber represented cell-free transmission events, and infected H9 cells detected from the bottom chamber represented total transmission events (cell-cell + cell free). Cell-cell transmission events were derived by subtracting the cell-free transmission events from the total transmission events. Western blots from harvested MDM cell lysates again showed that tetherin siRNA treatment successfully inhibited tetherin expression in MDMs in the Transwell plates (Figure 5E). siRNA silencing of tetherin in MDMs promoted cell-cell transmission from infected MDMs to H9 cells, with 4.5% ± 0.5% of H9 cells cocultured with tetherin siRNA-treated MDMs infected versus 2.8% ± 0.4% of H9 cells cocultured with control siRNA-treated MDMs (Figure 5F). These two methods yielded similar results, indicating that tetherin restricts cell-cell transmission from infected MDMs to T cells.

was shown to enhance particle release as established in prior experiments (Figure 6L).

Tetherin Upregulation in Infected MDMs Is Nef Dependent and Is Not a Direct Consequence of Type I Interferon Induction

Previous studies have reported that tetherin expression is highly interferon inducible in a large number of cell types (Neil et al., 2008). To understand the mechanism of tetherin upregulation in infected MDMs, we examined the relationship between type-I interferon production and tetherin expression in HIV-infected MDMs. We were able to detect IFN-α induction in supernatants from three out of six donors evaluated. The peak of IFN-α was detected later than the upregulation of tetherin, however, at day 8 postinfection (Figure 7A). Among the samples in which IFN-α was detected, the average peak concentration for NL4-3 and NLUdel-infected MDMs was 28.9 pg/ml and 16.5 pg/ml, respectively (Figure 7A), which would translate to 11.6 U/ml and 6.6 U/ml, according to the manufacturer's calibration. IFN-α was not detected in supernatants from MDMs with no infection (Figure 7A). We detected a much higher level of released IFN-α in the supernatant of poly(I:C)-treated MDMs (Figure 7A), and this correlated with an upregulation of tetherin on day 2 of poly(I:C) treated MDMs by western blotting (Figure 7B). In addition to IFN-α, we also tested the supernatants for IFN-β with an IFN-β ELISA. However, in all six donors that we tested for IFN-β, the level of IFN-β was below the detection limit of the assay (data not shown). The level and timing of IFN-α expression detected in our infected MDM cultures are consistent with a previous report (Szebeni et al., 1991). Because we did not detect production of IFN-α at early time points when tetherin was highly upregulated, IFN-α did not appear to be the cause for tetherin upregulation in infected MDMs. To further assess this, we supplied uninfected MDMs with exogenous human recombinant IFN-α in excess, and measured tetherin expression from the treated cells at various time points. Tetherin was not upregulated when the MDM culture was stimulated with 20 U/ml IFN-α, a level slightly higher than the highest we had measured in MDM culture supernatants (Figure 7C). We next treated MDMs with increasing amounts of IFN-α and found that the minimum amount required for tetherin upregulation was 50 U/ml (Figure 7D, Donor 2, lane 4) or 100 U/ml (Figure 7D, Donor 1, lane 5). Because we had demonstrated together with the Wu laboratory that HIV-1 Nef is involved in tetherin upregulation in dendritic cells (Coleman et al., 2011), we then infected MDMs with wild-type virus or virus lacking Nef expression (NLdeltaNef), and measured tetherin expression at various time points postinfection. Our result showed that in delta Nef-infected MDMs, tetherin upregulation was largely absent (Figure 7E), suggesting that HIV-1 Nef plays a role in tetherin upregulation in infected MDMs as it does in dendritic cells.

DISCUSSION

Membranous compartments harboring large collections of virus particles are frequently observed in HIV-1-infected macrophages. These compartments are variably referred to as virus-containing compartments (VCCs) or virus assembly compartments, because in addition to mature virions, immature virus particles as well as active budding viral structures are sometimes observed (Bennett et al., 2009; Orenstein et al., 1988). In this study, we have identified tetherin as a component of the VCC and provide evidence that tetherin plays a functional role in this compartment.

The subcellular distribution of tetherin in macrophages is quite distinct from that observed in other cell types. In epithelial cells such as HeLa, tetherin localizes to the plasma membrane, the TGN, and some early endosomal compartments, such as the recycling endosome compartment. In macrophages, we now demonstrate that tetherin is found largely on the plasma membrane and in two intracellular sites: the TGN and the CD81, CD9-enriched compartments where HIV virions accumulate (the VCC). HIV infection is not required to bring tetherin into this tetraspanin-enriched intracellular compartment, as indicated by the strong presence of tetherin colocalizing with CD81 and CD9 in uninfected MDMs. Instead, following HIV-1 infection, HIV particles accumulate in this tetherin/CD81/CD9-rich compartment, and CD63 and LAMP-1 are simultaneously enriched in the VCC. The enrichment of CD63 in the VCC is consistent with the previous observation that HIV alters the CD81+/CD9+ compartment and results in relocalization of CD63 into this compartment (Deneka et al., 2007). It was recently shown that tetherin functions by physically attaching to virus particles (Fitzpatrick et al., 2010; Hammonds et al., 2010; Perez-Caballero et al., 2009). Our data now indicate that physical tethering of particles occurs within the VCC as well. We found tetherin linking particles to the limiting membrane and linking particles to each other within the VCC.

Depletion of tetherin in macrophages created a markedly diminished VCC in macrophages, and a redistribution of the remaining intracellular viral particles into smaller, more peripheral compartments. This is consistent with a model in which tetherin is required for the formation of the VCC, or at least in trapping and retaining particles in this pre-existing compartment. Tetherin may trap particles peripherally, followed by endocytosis into the VCC, or tether and retain particles within the VCC as budding occurs within this compartment. We suggest from depletion studies that tetherin plays an integral role in the VCC, and that the upregulation of tetherin that follows HIV infection of MDMs is also an important factor in the formation of the VCC. The population of tetherin in the VCC appears to be completely distinct from the population in the TGN, and fails to colocalize with Vpu. This population may be more stable and resistant to degradation by Vpu than is the TGN-associated or actively recycling tetherin population.

Vpu was unable to completely counteract the upregulation of tetherin in macrophages, although it was able to limit the magnitude of tetherin upregulation, resulting in enhanced particle release compared with that seen with Vpu-deficient virus infection. Thus, the upregulation of tetherin in infected macrophages may result in enhanced sequestration of viruses in intracellular compartments, even when Vpu is expressed. The inability of Vpu to efficiently counteract tetherin in macrophages was especially evident when we observed an enhancement of particle release upon tetherin depletion, even in the case of Vpu-expressing viruses.

Miyagi and coworkers previously demonstrated that Vpu downregulates cell surface tetherin in macrophages (Miyagi

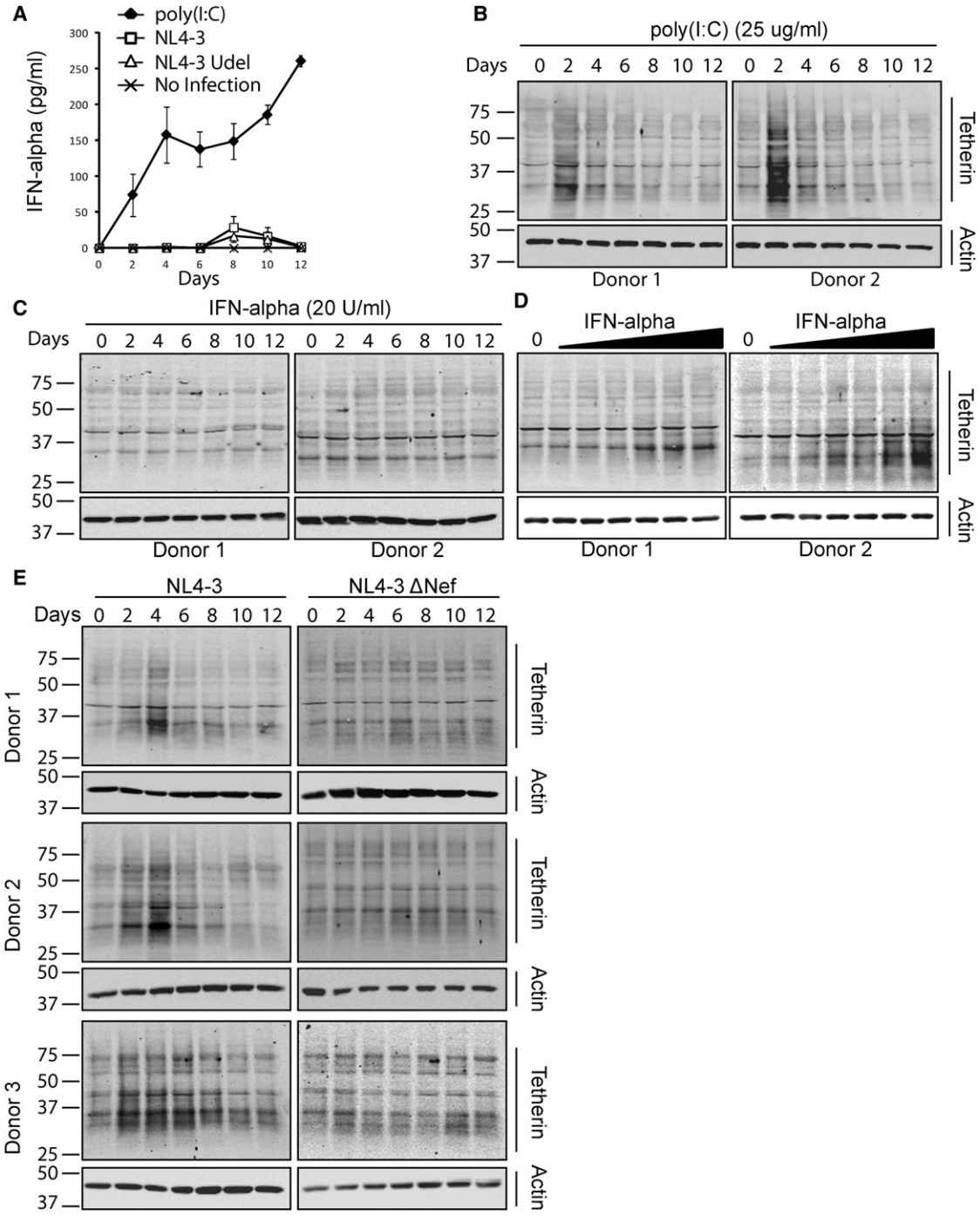

Figure 7. Mechanism of Tetherin Upregulation in Infected MDMs

(A) MDMs were infected with VSV-G-pseudotyped NL4-3 or VSV-G-pseudotyped NLUdel. MDMs from the same donors were stimulated with poly(I:C) by adding 25 ug/ml poly(I:C) in the cell cultures or were left untreated. IFN-α levels from the supernatants were measured by IFN-α ELISA. Error bars represent SD.

(B) Western blot of MDMs treated with 25 μg/ml high-molecular-weight poly(I:C). MDMs were harvested at indicated time points post-poly(I:C) treatment, lysed, and analyzed by western blotting using rabbit anti-tetherin or mouse anti-actin antiserum.

(C) Western blot of MDMs treated with 20 U/ml human recombinant IFN-α.

(D) MDMs were treated with 0, 10, 25, 50, 100, 500, or 1,000 U/ml human recombinant IFN-α. Twenty-four hours after the IFN-α treatment, MDMs were harvested and analyzed by western blotting.

(E) MDMs were infected with VSV-G-pseudotyped NL4-3 or VSV-G-pseudotyped NL4-3 delNef. Cell lysates were harvested at the indicated time points (days) and analyzed by western blot for tetherin and actin expression.

et al., 2009). In contrast, we demonstrate here that tetherin is upregulated following infection. The difference in these findings is likely attributable to the timing of the cell harvest for analysis following infection. We documented an increase in total tetherin levels for more than 6 days postinfection, after which tetherin levels return to baseline. Miyagi and coworkers harvested MDMs at 24 days postinfection, and did not report on earlier times postinfection (Miyagi et al., 2009).

Upregulation of tetherin in MDMs occurred at days 2–4 following HIV infection and did not correlate with release of α- or β-interferon. It is likely that intracellular pathogen recognition is occurring to stimulate this upregulation. Bego and colleagues have recently shown that stimulation of interferon regulatory factor 7 can upregulate tetherin expression in the absence of interferon signaling (Bego et al., 2012). It is intriguing to note that TRIM5α itself serves as a pathogen recognition receptor (Pertel et al., 2011), raising the possibility that tetherin could act in a similar manner. In our study, HIV Nef was required to elicit tetherin upregulation, as has been shown previously for both dendritic cells and macrophages (Schindler et al., 2010; Wu et al., 2004). Our results suggest that the high levels of induced tetherin in HIV-infected MDMs can explain the finding that even wild-type, Vpu-expressing virus in MDMs accumulates in the intracellular VCC. Vpu is unable to counteract tetherin efficiently in MDMs, leading to tetherin-mediated trapping of virus within the VCC.

VCCs in macrophages and in dendritic cells have been suggested to be sources of virus that are available to mediate cell-cell spread upon contact with the appropriate target cells (Gousset et al., 2008; Hubner et al., 2009; Lekkerkerker et al., 2006; Marsh et al., 2009; Piguet and Steinman, 2007; Yu et al., 2008). The presence of tetherin in VCCs in macrophages and the physical tethering of particles within this compartment is likely to have impact in how this compartment participates in cell-cell transmission events. We now demonstrate that the tethered virions within the VCC in macrophages are inhibited in infecting T lymphocyte target cells. Depletion of tetherin in HIV-infected MDMs led to significant increase in cell-cell transmission in our study. These results are in agreement with the findings of Casartelli and colleagues, who demonstrated that tetherin inhibits transmission of Vpu-deficient virus from infected cells and target T lymphocytes (Casartelli et al., 2010). Although macrophages were not examined in their study, they showed that transmission across the infectious synapse was inhibited, while polarization of viral particles to the contact site was not inhibited. Jolly and colleagues, in contrast, found that tetherin did not diminish cell-to-cell spread of virus (Jolly et al., 2010). Surprisingly, depletion of tetherin in their hands diminished the formation of the virologic synapse and decreased cell-cell spread of virus. They concluded that tetherin might in some circumstances actually enhance virus spread rather than inhibit spread. These authors were not examining MDMs, which may explain some of the contradictory conclusions of their study versus our study and the Casartelli study. It remains to be determined whether the large collections of tetherin-associated virions in human macrophages can be transmitted to target cells such as T lymphocytes, or whether the enhanced cell-cell transmission events seen upon tetherin knockdown are occurring from viruses assembling on the plasma membrane that escape tethering and subsequent delivery into intracellular compartments.

In summary, we demonstrate that tetherin is highly enriched at the site of HIV particle accumulation or assembly in infected macrophages, and that tetherin is a physical tether in this compartment as it is on the plasma membrane of T cells. Depletion of tetherin markedly diminished the size and altered the distribution of the VCC, suggesting that tetherin is required for its formation. Tetherin depletion in HIV-infected MDMs enhanced cell-cell transmission of HIV. Understanding further mechanistic details of the role of tetherin in HIV retention or release in macrophages, and of the reduced ability of Vpu to counteract tetherin in this cell type, will be important in efforts to eradicate potential reservoirs of HIV in infected individuals and in understanding cell-to-cell transmission events in vivo.

EXPERIMENTAL PROCEDURES

Preparation of Monocyte-Derived Macrophages

Peripheral blood was obtained from healthy volunteer donors according to a protocol approved by the Emory University Institutional Review Board (IRB). Peripheral blood mononuclear cells (PBMCs) were obtained from the buffy coat after Ficoll centrifugation and were allowed to adhere to plastic surface coated with poly-D-lysine (Sigma Aldrich, Saint Louis, MO, USA). Nonadherent PBMCs were washed away after 1 hr. Adherent monocytes were maintained in RPMI-1640 supplemented with 10% FBS, 100 ug/ml streptomycin, 100 U/ml penicillin, 2 mM glutamine, 1% sodium pyruvate, 1% nonessential amino acids, and 1U/ml GM-CSF (Cell Sciences, Canton, MA, USA). Monocytes were maintained in the supplemented media for 8 days for differentiation into macrophages, during which the media was replaced every 2 days. The purity of the macrophage population was assessed at day 10 by CD14 and CD68 staining and was on average greater than 93% (Figure S3).

Virus Stocks and Infections

Vesicular stomatitis virus G glycoprotein (VSV-G)-pseudotyped or wild-type HIV-NL4-3, HIV-NLUdel, and HIV-NL4-3-delNef virus stocks were generated by transfection of 293T cells. Some infections where noted were performed with BaL biological stocks using one tissue culture infectious dose ($TCID_{50}$) per cell.

siRNAs and Tetherin Knockdown

Tetherin siGENOME SMARTpool siRNA and control siGENOME nontargeting siRNA were purchased from Thermo Fisher Scientific (Dharmacon, Lafayette, CO, USA). Transfection of siRNAs into monocyte-derived macrophages (MDMs) was performed with the N-TER Nanoparticle siRNA Transfection System (Sigma Aldrich, Saint Louis, MO, USA). For tetherin knockdown experiments, freshly differentiated MDMs were treated with 100 nM tetherin siRNA or control siRNA three times at 72 hr, 48 hr, and 24 hr prior to virus infection. Supernatant and cell lysate from infected cells were harvested at days 0, 2, 4, 6, 8, 10, and 12 postinfection and stored at −80°C until analysis.

Image Acquisition and Analysis

Two imaging stations equipped for live-cell imaging were employed in this study. The first imaging station was a Nikon TE2000-U spinning-disc confocal fluorescence microscope with automated stage and Hamamatsu EM-CCD camera developed by Improvision under the control of the Volocity software. The second imaging station was a Deltavision imaging system developed by Applied Precision. The system was equipped with an Olympus IX70 microscope and a CoolSnap HQ2 digital camera under the control of the softWoRx software. Imaging processing and deconvolution were performed using softWoRx 3.7.0. Colocalization and partial colocalization measurements were quantified with the colocalization module of Volocity 5.2.1. For the tetherin knockdown experiments, colocalized pixels between Gag and CD9 were determined with the colocalization module of Volocity 5.5.1. The volume and the intensity of Gag among the colocalized pixels were calculated using the

measurements module of Volocity 5.5.1. Volocity 5.2.1, Volocity 5.5.1, Adobe Photoshop CS4, and Adobe Illustrator CS4 were used to analyze and adjust the images.

Immunofluorescence Microscopy

MDMs were washed with PBS and fixed in 4% paraformaldehyde for 12 min at RT. After fixation, cells were extensively washed including an overnight wash at 4°C. Cells were then permeabilized for 10 min with 0.2% Triton X-100 and blocked in Dako blocking buffer for 30 min. Primary and secondary antibodies were diluted in Dako antibody diluent to appropriate concentrations. In general, cells were stained in primary antibodies for 1.5 hr and in secondary antibodies for 45 min. DAPI was used to stain the nuclei of the cells. The coverslips were mounted in Gelvatol overnight and examined directly the next day.

Electron Microscopy

MDMs cultured on ACLAR embedding film (Ted Pella, Redding, CA, USA) were harvested at day 8, fixed in 4% paraformaldehyde for 1 hr followed by 4% paraformaldehyde + 0.1% glutaraldehyde, and embedded in Epon. Sections were etched with 5% H_2O_2 for 10 min and washed with deionized purified H_2O. Immunolabeling of tetherin was then performed using 6 nm gold beads with a protocol similar to that described previously (Hammonds et al., 2010). Images were obtained under a Hitachi H-7500 transmission electron microscope at 75KV.

Flow Cytometry

HeLa and MDM cultures were infected with VSV-G pseudotyped NL4-3 or NLUdel. Surface tetherin staining was performed with rabbit anti-tetherin antiserum as described (Hammonds et al., 2010), with additional staining as described in the Supplemental Experimental Procedures. Analysis was performed on a FACSCanto flow cytometer (BD Biosciences) and using FlowJo software (Treestar, Inc).

Cell-Cell Transmission Studies

Transmission of virus from infected MDMs was performed by gently centrifuging H9 cells onto MDMs in 24-well plates (method one) or by using Transwell culture plates with H9 cells and MDMs in contact (bottom chamber) or separated by a 0.4 μm filter (H9s in top chamber). For both methods, quantitation of transmission following the designated period of incubation was performed by counting CD3+, p24+ cells on a FACSCanto flow cytometer (BD Biosciences).

IFN-α ELISA and IFN-α Titration

IFN-α levels from MDM supernatants were measured by an IFN-α ELISA kit from Mabtech (Mariemont, OH, USA). IFN-β levels from MDM supernatants were detected by an IFN-β ELISA kit from PBL Interferon Source (Piscataway, NJ, USA).

Statistical Analysis

Statistical comparison between the groups was performed by unpaired t test using GraphPad Prism 5. Differences were considered statistically significant when $p \leq 0.05$.

SUPPLEMENTAL INFORMATION

Supplemental Information includes four figures, Supplemental Experimental Procedures, and Supplemental References and can be found with this article at http://dx.doi.org/10.1016/j.chom.2012.07.011.

ACKNOWLEDGMENTS

This work was supported by NIH AI058828 and NIH AI40338 and by funds from Children's Healthcare of Atlanta. The work was partly supported by the flow cytometry/cell sorting core of Children's Healthcare of Atlanta, by the Emory Center for AIDS Research (P30 AI050409), and by the Robert P. Apkarian Integrated Electron Microscopy Core Laboratory of Emory University. We thank the James B. Pendleton Charitable Trust for the gift of the Deltavision microscopy system.

Received: July 17, 2011
Revised: May 6, 2012
Accepted: July 19, 2012
Published: September 12, 2012

REFERENCES

Balliet, J.W., Kolson, D.L., Eiger, G., Kim, F.M., McGann, K.A., Srinivasan, A., and Collman, R. (1994). Distinct effects in primary macrophages and lymphocytes of the human immunodeficiency virus type 1 accessory genes vpr, vpu, and nef: mutational analysis of a primary HIV-1 isolate. Virology *200*, 623–631.

Bego, M.G., Mercier, J., and Cohen, E.A. (2012). Virus-activated interferon regulatory factor 7 upregulates expression of the interferon-regulated BST2 gene independently of interferon signaling. J. Virol. *86*, 3513–3527.

Bennett, A.E., Narayan, K., Shi, D., Hartnell, L.M., Gousset, K., He, H., Lowekamp, B.C., Yoo, T.S., Bliss, D., Freed, E.O., et al. (2009). Ion-abrasion scanning electron microscopy reveals surface-connected tubular conduits in HIV-infected macrophages. PLoS Pathog. *5*, e1000591. http://dx.doi.org/10.1371/journal.ppat.1000591.

Casartelli, N., Sourisseau, M., Feldmann, J., Guivel-Benhassine, F., Mallet, A., Marcelin, A.G., Guatelli, J., and Schwartz, O. (2010). Tetherin restricts productive HIV-1 cell-to-cell transmission. PLoS Pathog. *6*, e1000955. http://dx.doi.org/10.1371/journal.ppat.1000955.

Chu, H., Wang, J.J., and Spearman, P. (2009). Human immunodeficiency virus type-1 gag and host vesicular trafficking pathways. Curr. Top. Microbiol. Immunol. *339*, 67–84.

Coleman, C.M., Spearman, P., and Wu, L. (2011). Tetherin does not significantly restrict dendritic cell-mediated HIV-1 transmission and its expression is upregulated by newly synthesized HIV-1 Nef. Retrovirology *8*, 26.

Deneka, M., Pelchen-Matthews, A., Byland, R., Ruiz-Mateos, E., and Marsh, M. (2007). In macrophages, HIV-1 assembles into an intracellular plasma membrane domain containing the tetraspanins CD81, CD9, and CD53. J. Cell Biol. *177*, 329–341.

Douglas, J.L., Viswanathan, K., McCarroll, M.N., Gustin, J.K., Fruh, K., and Moses, A.V. (2009). Vpu directs the degradation of the human immunodeficiency virus restriction factor BST-2/Tetherin via a {beta}TrCP-dependent mechanism. J. Virol. *83*, 7931–7947.

Dube, M., Roy, B.B., Guiot-Guillain, P., Mercier, J., Binette, J., Leung, G., and Cohen, E.A. (2009). Suppression of Tetherin-restricting activity upon human immunodeficiency virus type 1 particle release correlates with localization of Vpu in the trans-Golgi network. J. Virol. *83*, 4574–4590.

Dube, M., Roy, B.B., Guiot-Guillain, P., Binette, J., Mercier, J., Chiasson, A., and Cohen, E.A. (2010). Antagonism of tetherin restriction of HIV-1 release by Vpu involves binding and sequestration of the restriction factor in a perinuclear compartment. PLoS Pathog. *6*, e1000856. http://dx.doi.org/10.1371/journal.ppat.1000856.

Finzi, A., Orthwein, A., Mercier, J., and Cohen, E.A. (2007). Productive human immunodeficiency virus type 1 assembly takes place at the plasma membrane. J. Virol. *81*, 7476–7490.

Fitzpatrick, K., Skasko, M., Deerinck, T.J., Crum, J., Ellisman, M.H., and Guatelli, J. (2010). Direct restriction of virus release and incorporation of the interferon-induced protein BST-2 into HIV-1 particles. PLoS Pathog. *6*, e1000701. http://dx.doi.org/10.1371/journal.ppat.1000701.

Gelderblom, H.R. (1991). Assembly and morphology of HIV: potential effect of structure on viral function. AIDS *5*, 617–637.

Goffinet, C., Allespach, I., Homann, S., Tervo, H.M., Habermann, A., Rupp, D., Oberbremer, L., Kern, C., Tibroni, N., Welsch, S., et al. (2009). HIV-1 antagonism of CD317 is species specific and involves Vpu-mediated proteasomal degradation of the restriction factor. Cell Host Microbe *5*, 285–297.

Gousset, K., Ablan, S.D., Coren, L.V., Ono, A., Soheilian, F., Nagashima, K., Ott, D.E., and Freed, E.O. (2008). Real-time visualization of HIV-1 GAG trafficking in infected macrophages. PLoS Pathog. *4*, e1000015. http://dx.doi.org/10.1371/journal.ppat.1000015.

Groot, F., Welsch, S., and Sattentau, Q.J. (2008). Efficient HIV-1 transmission from macrophages to T cells across transient virological synapses. Blood *111*, 4660–4663.

Habermann, A., Krijnse-Locker, J., Oberwinkler, H., Eckhardt, M., Homann, S., Andrew, A., Strebel, K., and Krausslich, H.G. (2010). CD317/tetherin is enriched in the HIV-1 envelope and downregulated from the plasma membrane upon virus infection. J. Virol. *84*, 4646–4658.

Hammonds, J., and Spearman, P. (2009). Tetherin is as tetherin does. Cell *139*, 456–457.

Hammonds, J., Wang, J.J., Yi, H., and Spearman, P. (2010). Immunoelectron microscopic evidence for Tetherin/BST2 as the physical bridge between HIV-1 virions and the plasma membrane. PLoS Pathog. *6*, e1000749. http://dx.doi.org/10.1371/journal.ppat.1000749.

Hubner, W., McNerney, G.P., Chen, P., Dale, B.M., Gordon, R.E., Chuang, F.Y., Li, X.D., Asmuth, D.M., Huser, T., and Chen, B.K. (2009). Quantitative 3D video microscopy of HIV transfer across T cell virological synapses. Science *323*, 1743–1747.

Iwabu, Y., Fujita, H., Kinomoto, M., Kaneko, K., Ishizaka, Y., Tanaka, Y., Sata, T., and Tokunaga, K. (2009). HIV-1 accessory protein Vpu internalizes cell-surface BST-2/tetherin through transmembrane interactions leading to lysosomes. J. Biol. Chem. *284*, 35060–35072.

Jolly, C., Booth, N.J., and Neil, S.J. (2010). Cell-cell spread of human immunodeficiency virus type 1 overcomes tetherin/BST-2-mediated restriction in T cells. J. Virol. *84*, 12185–12199.

Jouvenet, N., Neil, S.J., Bess, C., Johnson, M.C., Virgen, C.A., Simon, S.M., and Bieniasz, P.D. (2006). Plasma membrane is the site of productive HIV-1 particle assembly. PLoS Biol. *4*, e435. http://dx.doi.org/10.1371/journal.pbio.0040435.

Lekkerkerker, A.N., van Kooyk, Y., and Geijtenbeek, T.B. (2006). Viral piracy: HIV-1 targets dendritic cells for transmission. Curr. HIV Res. *4*, 169–176.

Le Tortorec, A., and Neil, S.J. (2009). Antagonism to and intracellular sequestration of human tetherin by the human immunodeficiency virus type 2 envelope glycoprotein. J. Virol. *83*, 11966–11978.

Manders, M.M., Verbeek, P.J., and Aten, J.A. (1993). Measurement of co-localization of objects in dual colour confocal images. J. Microsc. *169*, 375–382.

Mangeat, B., Gers-Huber, G., Lehmann, M., Zufferey, M., Luban, J., and Piguet, V. (2009). HIV-1 Vpu neutralizes the antiviral factor Tetherin/BST-2 by binding it and directing its beta-TrCP2-dependent degradation. PLoS Pathog. *5*, e1000574. http://dx.doi.org/10.1371/journal.ppat.1000574.

Marsh, M., Theusner, K., and Pelchen-Matthews, A. (2009). HIV assembly and budding in macrophages. Biochem. Soc. Trans. *37*, 185–189.

Masuyama, N., Kuronita, T., Tanaka, R., Muto, T., Hirota, Y., Takigawa, A., Fujita, H., Aso, Y., Amano, J., and Tanaka, Y. (2009). HM1.24 is internalized from lipid rafts by clathrin-mediated endocytosis through interaction with alpha-adaptin. J. Biol. Chem. *284*, 15927–15941.

Mitchell, R.S., Katsura, C., Skasko, M.A., Fitzpatrick, K., Lau, D., Ruiz, A., Stephens, E.B., Margottin-Goguet, F., Benarous, R., and Guatelli, J.C. (2009). Vpu antagonizes BST-2-mediated restriction of HIV-1 release via beta-TrCP and endo-lysosomal trafficking. PLoS Pathog. *5*, e1000450. http://dx.doi.org/10.1371/journal.ppat.1000450.

Miyagi, E., Andrew, A.J., Kao, S., and Strebel, K. (2009). Vpu enhances HIV-1 virus release in the absence of Bst-2 cell surface down-modulation and intracellular depletion. Proc. Natl. Acad. Sci. USA *106*, 2868–2873.

Montaner, L.J., Crowe, S.M., Aquaro, S., Perno, C.F., Stevenson, M., and Collman, R.G. (2006). Advances in macrophage and dendritic cell biology in HIV-1 infection stress key understudied areas in infection, pathogenesis, and analysis of viral reservoirs. J. Leukoc. Biol. *80*, 961–964.

Neil, S.J., Zang, T., and Bieniasz, P.D. (2008). Tetherin inhibits retrovirus release and is antagonized by HIV-1 Vpu. Nature *451*, 425–430.

Nydegger, S., Foti, M., Derdowski, A., Spearman, P., and Thali, M. (2003). HIV-1 egress is gated through late endosomal membranes. Traffic *4*, 902–910.

Ono, A., and Freed, E.O. (2004). Cell-type-dependent targeting of human immunodeficiency virus type 1 assembly to the plasma membrane and the multivesicular body. J. Virol. *78*, 1552–1563.

Orenstein, J.M., Meltzer, M.S., Phipps, T., and Gendelman, H.E. (1988). Cytoplasmic assembly and accumulation of human immunodeficiency virus types 1 and 2 in recombinant human colony-stimulating factor-1-treated human monocytes: an ultrastructural study. J. Virol. *62*, 2578–2586.

Pelchen-Matthews, A., Kramer, B., and Marsh, M. (2003). Infectious HIV-1 assembles in late endosomes in primary macrophages. J. Cell Biol. *162*, 443–455.

Perez-Caballero, D., Zang, T., Ebrahimi, A., McNatt, M.W., Gregory, D.A., Johnson, M.C., and Bieniasz, P.D. (2009). Tetherin inhibits HIV-1 release by directly tethering virions to cells. Cell *139*, 499–511.

Pertel, T., Hausmann, S., Morger, D., Zuger, S., Guerra, J., Lascano, J., Reinhard, C., Santoni, F.A., Uchil, P.D., Chatel, L., et al. (2011). TRIM5 is an innate immune sensor for the retrovirus capsid lattice. Nature *472*, 361–365.

Piguet, V., and Steinman, R.M. (2007). The interaction of HIV with dendritic cells: outcomes and pathways. Trends Immunol. *28*, 503–510.

Raposo, G., Moore, M., Innes, D., Leijendekker, R., Leigh-Brown, A., Benaroch, P., and Geuze, H. (2002). Human macrophages accumulate HIV-1 particles in MHC II compartments. Traffic *3*, 718–729.

Rollason, R., Korolchuk, V., Hamilton, C., Schu, P., and Banting, G. (2007). Clathrin-mediated endocytosis of a lipid-raft-associated protein is mediated through a dual tyrosine motif. J. Cell Sci. *120*, 3850–3858.

Schindler, M., Rajan, D., Banning, C., Wimmer, P., Koppensteiner, H., Iwanski, A., Specht, A., Sauter, D., Dobner, T., and Kirchhoff, F. (2010). Vpu serine 52 dependent counteraction of tetherin is required for HIV-1 replication in macrophages, but not in ex vivo human lymphoid tissue. Retrovirology *7*, 1.

Schubert, U., Clouse, K.A., and Strebel, K. (1995). Augmentation of virus secretion by the human immunodeficiency virus type 1 Vpu protein is cell type independent and occurs in cultured human primary macrophages and lymphocytes. J. Virol. *69*, 7699–7711.

Sherer, N.M., Lehmann, M.J., Jimenez-Soto, L.F., Ingmundson, A., Horner, S.M., Cicchetti, G., Allen, P.G., Pypaert, M., Cunningham, J.M., and Mothes, W. (2003). Visualization of retroviral replication in living cells reveals budding into multivesicular bodies. Traffic *4*, 785–801.

Szebeni, J., Dieffenbach, C., Wahl, S.M., Venkateshan, C.N., Yeh, A., Popovic, M., Gartner, S., Wahl, L.M., Peterfy, M., Friedman, R.M., et al. (1991). Induction of alpha interferon by human immunodeficiency virus type 1 in human monocyte-macrophage cultures. J. Virol. *65*, 6362–6364.

Van Damme, N., Goff, D., Katsura, C., Jorgenson, R.L., Mitchell, R., Johnson, M.C., Stephens, E.B., and Guatelli, J. (2008). The interferon-induced protein BST-2 restricts HIV-1 release and is downregulated from the cell surface by the viral Vpu protein. Cell Host Microbe *3*, 245–252.

Wu, L., Martin, T.D., Han, Y.C., Breun, S.K., and KewalRamani, V.N. (2004). Trans-dominant cellular inhibition of DC-SIGN-mediated HIV-1 transmission. Retrovirology *1*, 14.

Yu, H.J., Reuter, M.A., and McDonald, D. (2008). HIV traffics through a specialized, surface-accessible intracellular compartment during trans-infection of T cells by mature dendritic cells. PLoS Pathog. *4*, e1000134. http://dx.doi.org/10.1371/journal.ppat.1000134.